Feasibility of instrumental detection of meteorites in Antarctica

Daniel Faber

Student #67742352

Postgraduate Certificate in Antarctic Studies

University of Canterbury

Summary

Currently the most effective method of detecting meteorites in Antarctica is by eye. An investigation has been made of the feasibility of locating Antarctica meteorites by use of magnetic and/or electromagnetic means, as commonly used in other areas of geophysics.

It is found that Ground Penetrating Radar (GPR) is a promising candidate for detection of solid bodies buried within the ice to at depths around 1m, and would thus be an effective approach to locating meteorites at the bottom of cryoconites. The expected detection limits of a GPR system has been calculated for the conditions expected in Antarctic meteorite stranding sites with cryoconites, and a study of the optimum instrument configuration was performed.

For meteorites very near to the surface, such as under a thin cover of snow, GPR is limited by surface clutter. Magnetometers are proposed as a more effective detection method, and an initial look at the important parameters of a magnetometer-bases system was undertaken to determine if further study is warranted in that area.

The advantages and disadvantages of GPR is discussed, and compared to the effectiveness of the current visual detection method. While it is concluded that the GPR systems (and potentially magnetometer) will allow the detection of large numbers of meteorites that are currently going unnoticed, it is also noted that the search efficiency and collection rates would likely not improve using these technologies, and thus they are unlikely to be implemented in the near future.

Background

Searching for meteorites in Antarctica has been highly productive, with 36,533 meteorites recovered and cataloged to date. This equates to 70% of the global total of 52,515 known meteorites as of 15 February 2011 (1).

The vast majority of these meteorites have been recovered from the ablation zones known as "blue ice", at high altitude along the margins of the polar plateau, by expedition teams of up to dozens of people walking over the ice and locating the meteorites visually (see Figure 1). The meteorites are brought to the surface by the slow movement of the ice and the slow ablation of the surface by the high wind and dry Antarctic air. However, locating meteorites visually requires the ice surface to be clear of snow that can obscure the meteorites, and for the meteorites to be sitting at or above the surface.

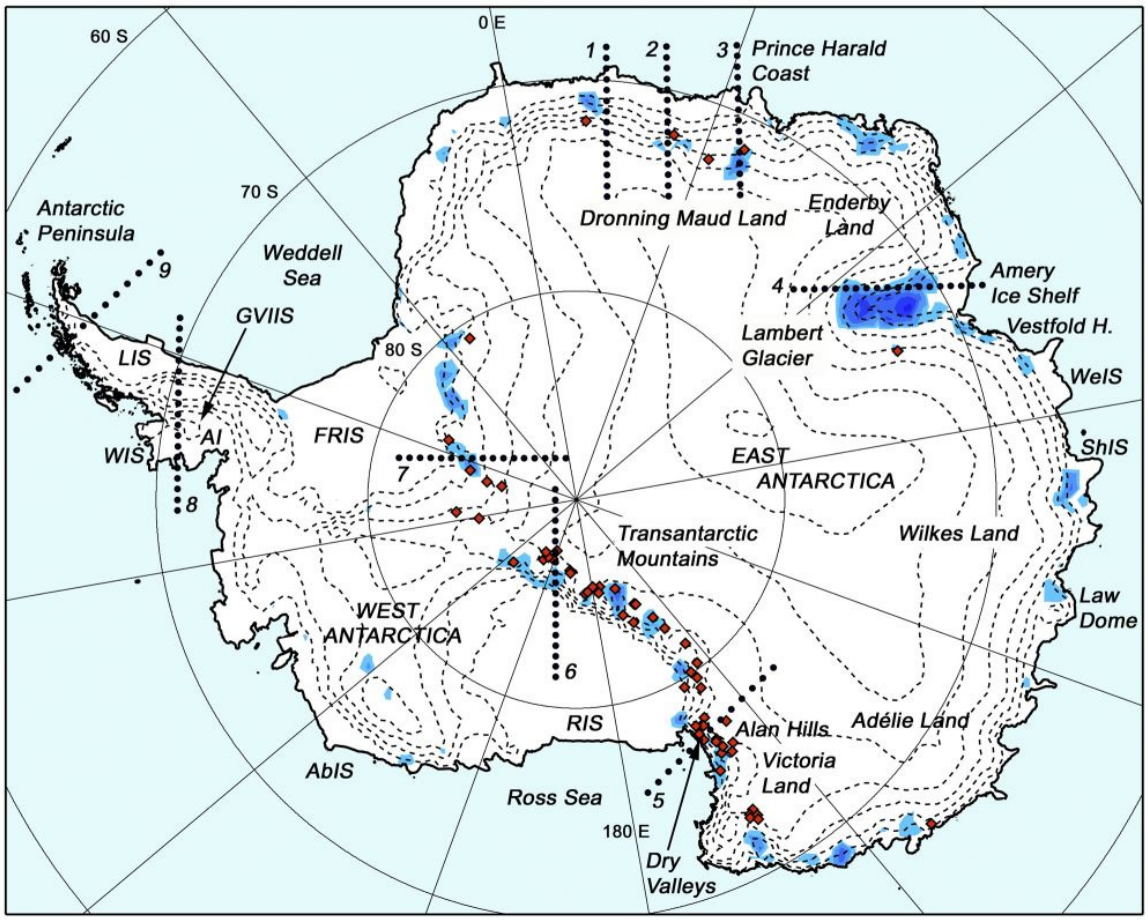

Figure 1 Map of Antarctica with blue areas indicating regions with >10% blue ice. Red diamonds indicate known meteorite stranding sites. Elevation contours are every 500 m (2)

The most significant limiting factor on Antarctic meteorite recovery efforts is the logistic cost of supporting large search teams (3). Currently the most effective meteorite detector for Antarctic meteorite searches is the human eye. No available electronic system can compete with a visual search that easily recognizes features that are unique or out of

place. The dark, cm-sized meteorite can be identified by eye at distances of up to 100 meters on the light colored ice, in the absence of terrestrial rocks (3).

The US Antarctic Search for Meteorites (ANSMET) program has fielded and tested a number of instruments from simple metal detectors to a meteorite hunting robot (NOMAD) equipped with multiple sensors and intelligent processing algorithms (4), with limited success. One of the major issues is the presence of terrestrial rocks in many meteorite stranding sites. For example, of the 5900 specimens recovered from meteorite stranding surfaces in the Walcott Névé region all but a few hundred were recovered from regions rich in terrestrial rock (3).

Targets

Antarctic meteorites vary in size, being typically 1cm to 10 cm in diameter. While all Antarctic meteorites located to date have been on the surface, the potential exists to use geophysical techniques to locate near-surface meteorites at a depth in ice ranging from surface (covered by a thin layer of snow) down to several meters. Greater detection depth is a desirable outcome, as the meteorites can sink some depth into cryoconites when the ambient temperature is close to zero Celsius, however recovery may not be feasible.

State of the art

The "Robotic Antarctic Meteorite Search Project" used the Nomad robotic wheeled vehicle has been deployed in Antarctica in 1997 and 1998, as described in (9), and in 2000, described in (10). A panoramic camera was used for initial detection and location of rocks on ice, under remote operator control. A high resolution camera and spectrometer were used to differentiate between terrestrial rocks and meteorites, in situ. Effectively this was attempting to replace a visual survey by human eyes. In January 2000 the Nomad robot found and classified, in situ, five indigenous meteorites and dozens of terrestrial rocks (4), however the program was not considered competitive with a human visual search, and was not continued.

It is generally considered by the leadership of the most prolific Antarctic meteorite search that, "In spite of the sophistication of [instruments for meteorite detection] approach, high technology is unlikely to supplant visual searches for several reasons. First, many technological sensors sort potential specimens in ways antithetical to the value of the Antarctic collection. For example, while metal detectors can be routinely used to locate iron, stony iron and ordinary chondrite meteorites, many of the most scientifically valuable Antarctic meteorites are igneous specimens that bear few ferromagnetic minerals and thus are indistinguishable from terrestrial rocks. Second, while the speed of modern computer processors and robotic systems is growing dramatically, the human mind's ability to integrate a scene and pick out key elements remains vastly superior." (3). It is none the less useful to consider alternative detection methods and technologies that may prove useful in the future.

Ground Penetrating Radar

The GPR technique is used to locate and characterize near-surface objects and features, with a maximum depth of detection of a few tens of meters (16). GPR relies of scattering or reflection of radio waves from the interface between two materials with different electrical properties. A pulse of radio waves is directed into the ground and energy that is scattered back towards the antenna from any objects or layers can be detected a short time later. The time delay between transmission and detection is proportional to the distance of the object from the antenna. Detection requires on sufficient reflected power.

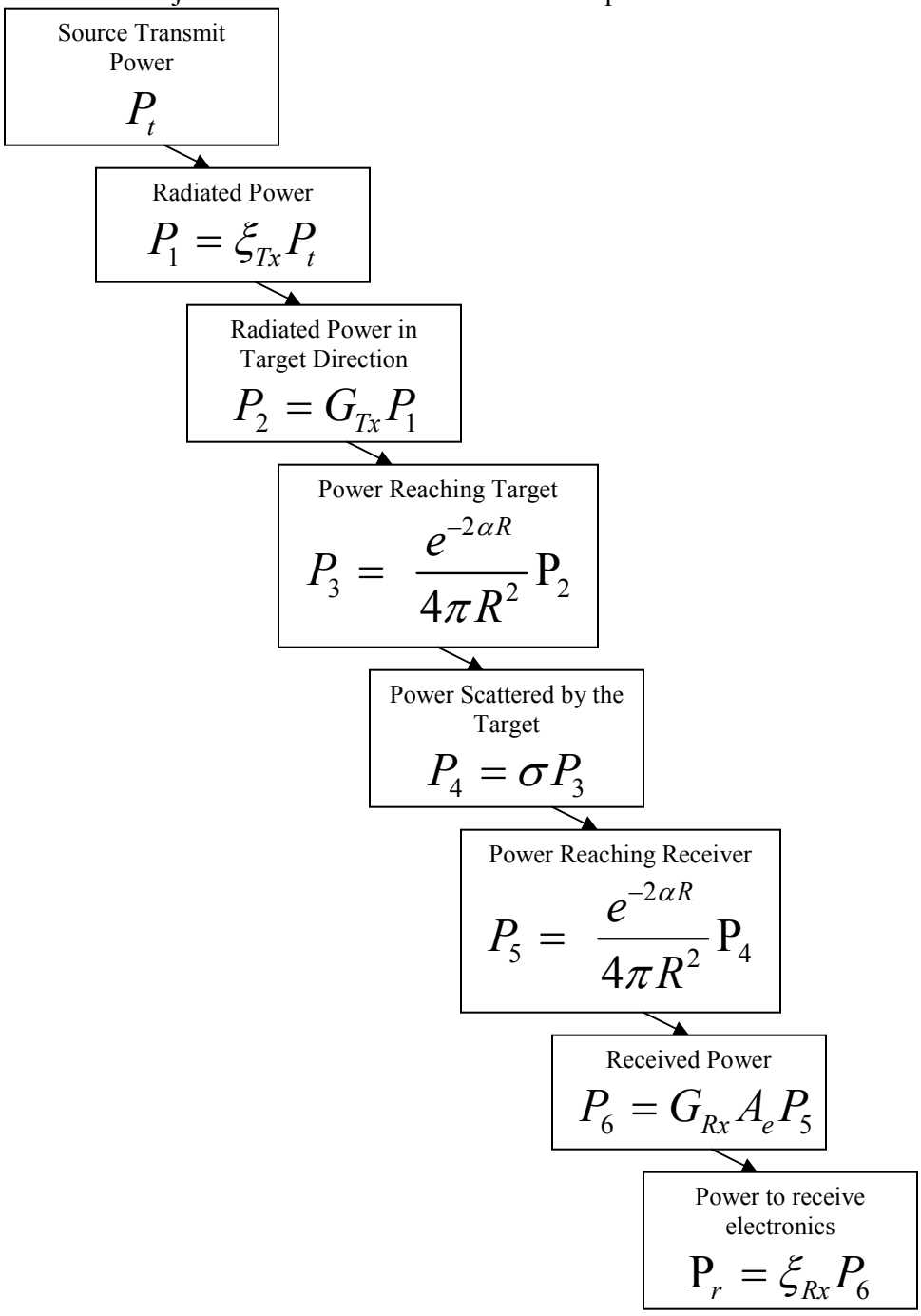

Figure 2 Method to calculate the return signal from a radar target (19)

The method of determining received signal power, as indicated in Figure 2, yields in the following equation:

$$P_r = \frac{P_t \xi^2 G^2 \sigma e^{-4\alpha R}}{16\pi^2 R^4}$$

Where:

P_r = peak received power

P_t = peak transmitted power

ξ = antenna & Cabling Efficiency

G = antenna gain

σ = radiation cross-section of the target

α = Attenuation constant of the transmission medium

R = range from the antenna to the target

The crucial parameter for delectability of a target is the ratio of the received signal power to the noise of the system:

$$SNR = \frac{P_r}{N}$$

Where:
N = system noise

Analysis

Peak Transmit Power
Peak transmit power on the order of ten kilowatts is under development (16), (36), (37), and systems are in use operating at over 1kW, however they do not appear to be commercially available. We shall assume P_t = 1kW, in order to ensure that the system we are specifying can in be built in practice.

Antenna & Cabling Efficiency
Antenna and cabling efficiency of up to 50% has been theorized in literature (38), however because many antennas are resistively loaded to prevent them from ringing when shock excited (to reduce cross-coupling of the transmit and receive signals), the

efficiency is often compromised (39). We shall use a conservative value of $\xi_{Tx} = \xi_{Rx} =$ 10%.

Antenna Gain

Antenna gain describes the directivity of the radiation pattern created by the antenna geometry, as shown diagrammatically in Figure 3. It is usually calculated at a sufficient distance form the antenna such that the radio wave fronts are effectively parallel, in a region called the "far field". However, in GPR the distance from the antenna to the targets is around 1m, and the typical wavelength of GPR systems is 3m to 30cm (100MHz to 1GHz). This means we are operating in the near field of the antenna, and the typical far-field equations do not apply, making the calculation of antenna gain somewhat complex. Antenna gains between 1 and 13 dB has been reported (both from measurement and simulation) for various GPR antennas (21), (23), (24), (25), (26), (27), (28), (29), (30). We will use a gain of 6dB for our calculations, as this appears to be achievable in practice, or a 4:1 ratio of effective isotropic radiated transmit power to actual transmit power.

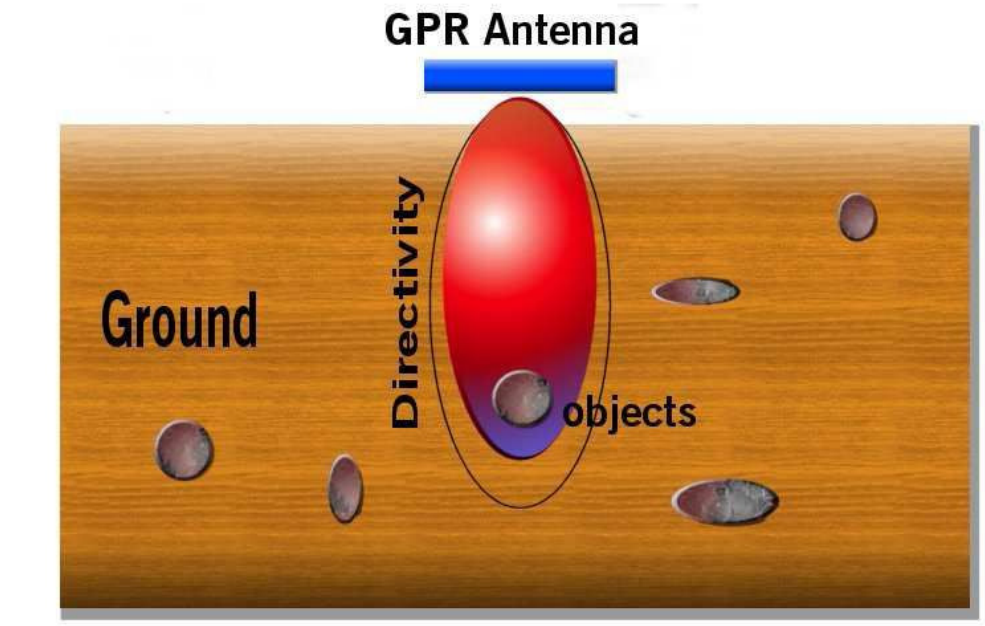

Figure 3 Directivity of GPR antennas (25)

Radiation Cross Section of target

The radiation cross section of a target can be viewed as a comparison of the strength of the reflected signal from a target to the reflected signal from a perfectly smooth and perfectly reflective sphere of cross-sectional area of $1m^2$. When the wavelength is less than the radius of the target, for a spherical target the radar cross section $\sigma = \pi r^2$, where r is the radius of the sphere in meters (22). Considering our meteorite targets, with diameters down to 1cm (r = 0.005m), this assumption will not hold unless we are operating above 60 GHz which is higher that typical radar systems. At longer

wavelengths (lower frequencies), below 10GHz, Rayleigh scattering is dominant, as region as shown in Figure 4, and the radiation cross section can thus be calculated as $\sigma = 113.8 \times \pi^5 \times r^6 / \lambda^4$, where λ is wavelength, in meters. For frequencies in the resonant region between 10 and 60 GHz a conservative approach is used, assuming that the cross-section is equal to the minimum (point B in Figure 4), or $\sigma = 0.26\pi r^2$.

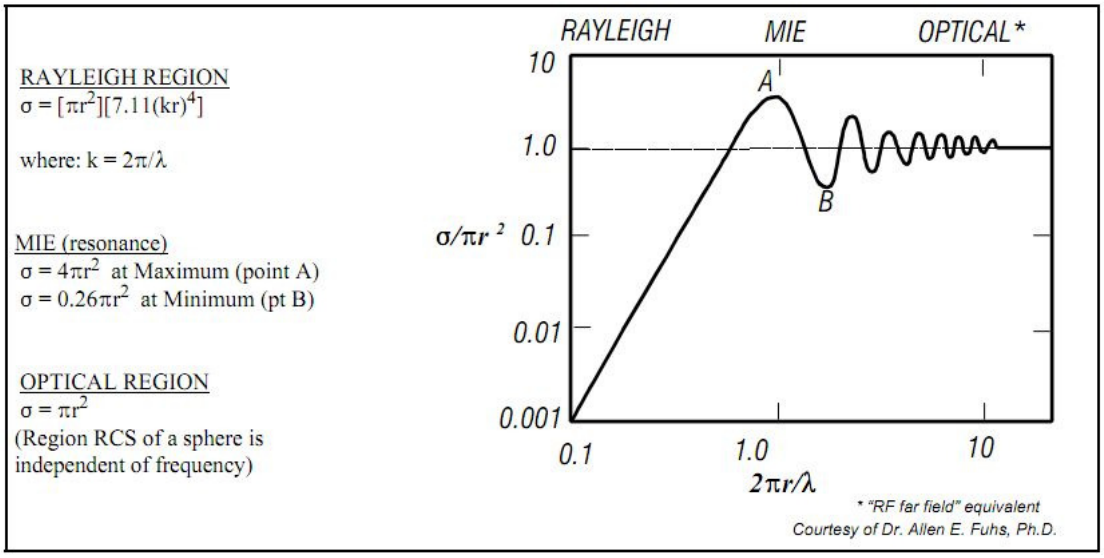

Figure 4 Radar Cross Section of a Sphere (22)

This analysis assumes a that the target has significantly higher conductivity than the medium in which it is embedded. This is a reasonable starting assumption for meteorites in ice.

Further investigation is recommended. It is noted that the majority of targets sought using subsurface radar methods are nonmetallic so that their scattering cross-section is dependent upon the properties of the surrounding dielectric medium (21).

Attenuation constant of the transmission medium

The attenuation constant, α, can be calculated based on the electrical properties of the ice using the equation (20):

$$\alpha = \frac{1690\sigma_c}{(K')^{\frac{1}{2}}} \quad \text{(dB/m)}$$

And

$$\sigma_c = \sigma_{dc} + \varpi K''\varepsilon_0 = \varpi K'''\varepsilon_0$$

These equations are approximations, and require that $\sigma_c / \varpi K'\varepsilon_0$ is much less than 1 (20).

Where:

σ_c is the complex conductivity of the transmission medium (ice). While it is reported in literature as 10^{-5} S/m at 100 MHz (21), we will use the method above to calculate the conductivity over a range of frequencies.

σ_{dc} is the DC conductivity. It has been variously reported as between 10^{-7} and 10^{-9} S/m (40), (41) in pure ice. However, even with a small amount of impurities can change the conductivity significantly (40) as shown in Figure 5. Considering the ice in the region of cryoconites is likely to be cracked, and the potential for liquid water trapped within those cracks, it is only reasonably to use a reported conductivity for such a situation as a conservative estimate, that being 10^{-4} S/m (21).

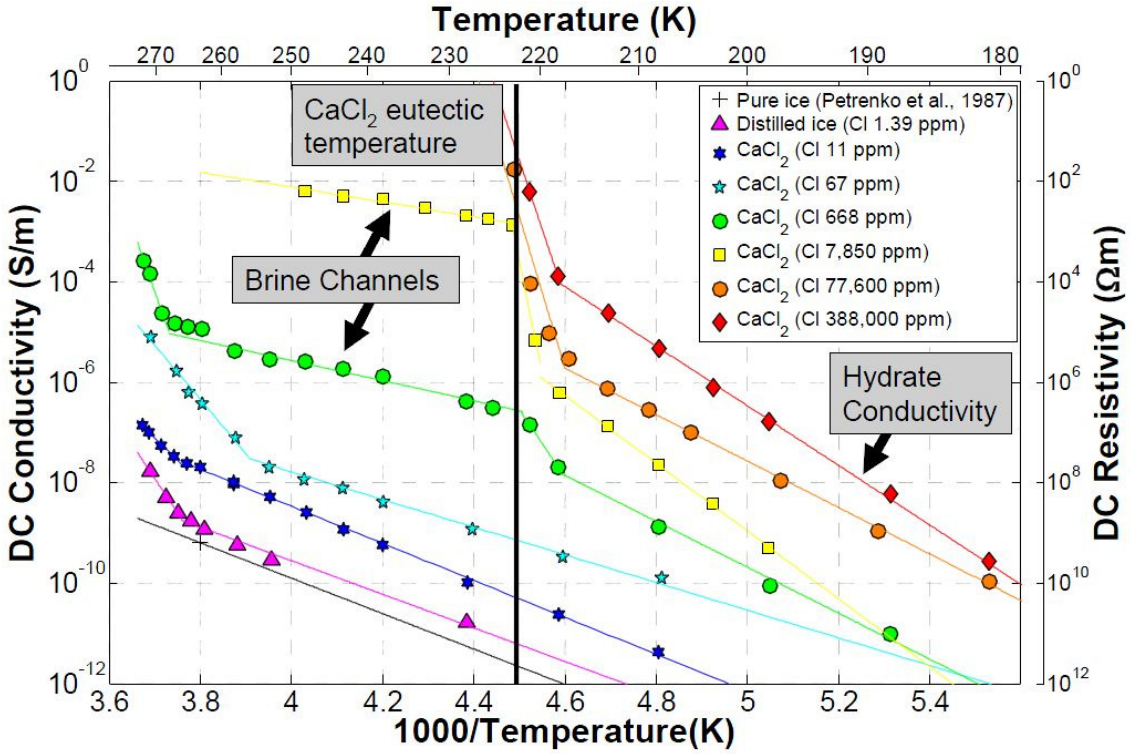

Figure 5 Ice DC Conductivity versus Temperature (40)

ω is the angular frequency = $2\pi f$ (rad.s^{-1}), where f is the radar center frequency in Hz

K' is the real component of the complex dielectric constant, and has been measured to be approximately constant over a large frequency range, with a value of 3.17 from10 MHz to tens of GHz (32), (34), (35) and 3.15 at higher frequencies (33). For these calculations we will use a value of 3.17 across all frequencies.

K" is the frequency-dependent loss associated with the relaxation response phenomena

K"' is the imaginary or loss part of the dielectric constant. It has been variously reported for ice to be between 6×10^{-4} and 9.0×10^{-3} (42), (43), (44). We will use K"' = 3×10^{-3} in our calculations. Importantly of our purposes the loss part of the dielectric constant does not appear to vary significantly with frequency.

ε_0 is the Free space permittivity = 8/85E-12 F/m

We note that σ_c has been reported as 1×10^{-5} S/m at 100 MHz (20), our calculation of 1.67×10^{-5} S/m at 100 MHz is slightly more conservative, as expected.

Target Range

We are interested in meteorites that are below the surface, yet could still be extracted by a search team practically this limits the depth to a few meters in a cryoconites, and perhaps 1 meter in solid ice. We will use this value for our calculations.

An analysis of the expected depth of meteorites within cryoconites would be useful to determine the most applicable locations to deploy this method. The depth of a cryoconite will depend on the maximum air temperature experienced at any location and on the size of the meteorite. Equations for this calculation can be developed from the thermal energy balance at the bottom of the hole, and are developed for dust particles in (45), however a thorough analysis is beyond the scope of this report.

System noise

For a signal to be detected, it must be obvious above the background noise that is seen by the receiver. The noise can be calculated as:

$N = kT_0B(NF)$

Where:

N = noise seen by the receiver.

k = Boltzmann's Constant = 1.38×10^{-23} J/K

T_0 = Absolute temperature (K) of the receiver input, which we shall conservatively assume to be 290K. While the ambient temperature may be significantly lower, the electronics and RF components will be producing significant heat, likely inside an insulated container. This is also in line with the IEEE standard for specifying system performance.

B = Receiver Bandwidth (Hz) in GPR systems can be up to 1 GHz (10^9 Hz). We will assume the bandwidth is equal to the smaller of 1GHz (10^9 Hz) or half of the nominal operating frequency.

The main advantage of using such a broad bandwidth for GPR is increased vertical resolution (also known as down-range or depth resolution), which is closely related to the radar operational bandwidth. $\Delta v = \frac{c}{2 * \Delta f}$

where Δv is the vertical resolution of the system, c is the velocity of an electromagnetic signal in vacuum, and Δf is the bandwidth used by the system." ([5] in (18)). A 1GHz bandwidth yields a 15cm vertical resolution, which is deemed necessary in deciding how to retrieve the meteorite once it has been detected.

NF = Noise Figure of the receiver, which is typically dominated by Johnson Noise for GPR systems, which is the noise generated by the thermal motion of the electrons inside the electronics. Modern GPR systems have solid state amplifiers at their input stage, which have a typical Noise Figure of 4.0 (usually expressed as 6dB) (22).

From these assumptions we calculate the noise:

$N = 1.6\times10^{-11}$ Watts for a 1GHz bandwidth receiver.

System Performance

Returning to the equation for received signal power and SNR, the following spreadsheet (Table 1) was created to perform the calculation at multiple frequencies:

$$P_r = \frac{P_t \xi^2 G^2 \sigma e^{-4\alpha R}}{16\pi^2 R^4}$$

Frequency	f	Hz GHz	1.00E+08 0.1	1.00E+09 1.0	6.50E+09 6.5	1.00E+10 10.0	1.00E+11 100.0
Transmit Power	P_t	W	1000	1000	1000	1000	1000
Efficiency	H		10%	10%	10%	10%	10%
Antenna Gain	G		4.00	4.00	4.00	4.00	4.00
Radius of Target	r	m	0.005	0.005	0.005	0.005	0.005
Speed of Light	c	m/s	3.00E+08	3.00E+08	3.00E+08	3.00E+08	3.00E+08
Wavelength	λ	m	3.000	0.300	0.046	0.030	0.003
	2πr/λ		0.010	0.105	0.681	1.047	10.472
	σ(Rayleigh)		6.72E-12	6.72E-08	1.20E-04	6.72E-04	6.72E+00
	σ(MIE)		2.04E-05	2.04E-05	2.04E-05	2.04E-05	2.04E-05
	σ(Optical)		7.85E-05	7.85E-05	7.85E-05	7.85E-05	7.85E-05
Scattering Type			Rayleigh	Rayleigh	Rayleigh	MIE	Optical
Radar Cross Section	σ	m2	6.72E-12	6.72E-08	1.20E-04	2.04E-05	7.85E-05
DC Conductivity	σdc	S/m	1.00E-04	1.00E-04	1.00E-04	1.00E-04	1.00E-04
Real component of dielectric constant	K'		3.17	3.17	3.17	3.17	3.17
Loss component of dielectric constant	K'''		3.00E-03	3.00E-03	3.00E-03	3.00E-03	3.00E-03
Permittivity of free space	εo	F/m	8.85E-12	8.85E-12	8.85E-12	8.85E-12	8.85E-12
Angular frequency	ω	rad/s	6.28E+08	6.28E+09	4.08E+10	6.28E+10	6.28E+11
check validity of attenuation			5.67E-03	5.67E-04	8.72E-05	5.67E-05	5.67E-06
Complex Conductivity	σc	S/m	1.67E-05	1.67E-04	1.08E-03	1.67E-03	1.67E-02
Attenuation Constant	a	dB/m	0.02	0.16	1.03	1.58	15.84
Distance to Target	R	m	1	1	1	1	1
Receive Power	Pr	W	6.39E-12	3.61E-08	1.98E-06	3.66E-08	2.41E-32
Boltzman's Constant	k	J/K	1.38E-23	1.38E-23	1.38E-23	1.38E-23	1.38E-23
Temperature	To	K	290	290	290	290	290
Bandwidth	B	Hz	5.00E+07	5.00E+08	1.00E+09	1.00E+09	1.00E+09
Noise Figure	NF		4.00	4.00	4.00	4.00	4.00
Noise Power	N	W	8.00E-13	8.00E-12	1.60E-11	1.60E-11	1.60E-11
Signal-to-Noise Ratio	SNR		7.98	4510.98	123400.52	2288.06	0.00

Table 1 Calculation of SNR at various frequencies

The SNR is shown against frequency in Figure 6 to peak at 65GHz. Above this frequency the attenuation losses are the limiting factor, and below this frequency the radiation cross section is the limiting factor.

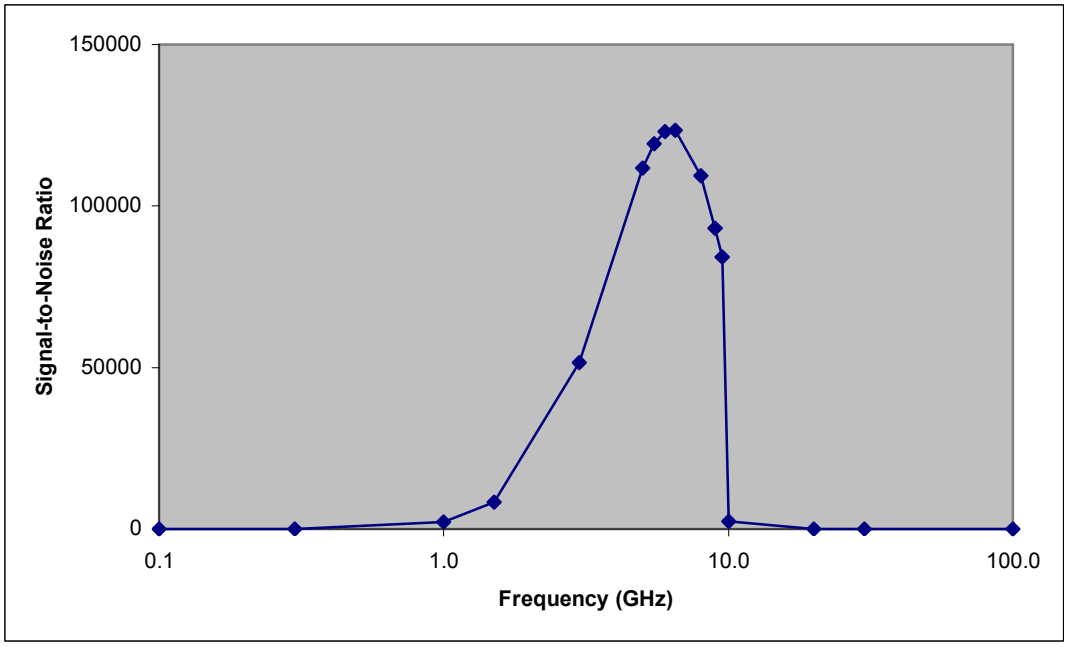

Figure 6 SNR versus Frequency for detection of 1cm diameters objects at 1m depth in glacial ice

Detection limits

Typically a positive detection of an anomaly (ie. a meteorite) is defined as occurring whenever the received power is higher than a threshold.

Measuring system performance as the Signal to Noise Ratio (SNR), we can statistically estimate true and false detection probabilities. The SNR threshold for reporting a positive detection will occasionally provide a false detection due to the random nature of the noise. Every time that a false positive detection is made, the surveyor team will waste time searching for the non-existent meteorite by repeating the search in that area. Assuming that we are taking a GPR measurement every 0.2m, it would require a grid of 5000×5000 readings to cover 1 km^2, or 25 million readings. The ANSMET average is about 10 meteorites per square kilometer (31) which we will assume to be the distribution in our theoretical search area, therefore an SNR of 5 would result in 7.1 false readings for 10 true readings, or 40% false positive readings, assuming that each true reading is above the threshold of SNR = 5. A threshold at SNR = 6 would produce 0.024 false positives per km^2, or 0.24% false positives, which would appear to be an acceptable level. These results are summarized in Table 2

SNR	False Positive		
	Per million measurements	Per square kilometer	% false positives, assuming 10 meteorites per km^2
1	159,000	3.975,000	100.0 %
2	22,800	570,000	100.0 %
3	1,350	33,750	99.97 %
4	30	750	98.7 %
5	0.285	7.125	41.6 %
6	0.000986	0.02465	0.25 %

Table 2 False positive detections for various SNR thresholds

Integration time

The signal-to-noise ratio can be reduced by averaging many measurements; however this increases the time to take a combined measurement and thus reduces the survey speed. As we required 25 million sample points to cover 1km^2, it is not feasible to repeat measurements in order to improve the SNR.

Survey Speed

In order for a survey technique to be useful it must be possible to perform it at a similar or faster speed than the current visual search techniques. Current surveys of areas that are free of terrestrial rocks are performed on skidoos moving at a fast walking speed, or even a running speed, with a skidoo separation of 30m. While it should be possible to design a GPR system with multiple antenna heads on a 30m boom to trail behind a skidoo, the practicality of towing this system at speed over rough ice and sastrugi may be difficult. At this stage this is seen as a design challenge, not a show-stopper.

More difficult will be providing 1kW of RF power to multiple detector heads (antenna pairs). A 30m boom may have 60 to 120 detector heads, requiring the transmit power to be dropped by similar factor. As the SNR is proportional to transmit power, a quick glance at the calculated SNR in Figure 6 shows that this would be an acceptable reduction. Again, at this stage this is seen as a design challenge, not a show-stopper.

Sub-surface Clutter

One feather of the potential search areas that has been ignored in this calculation is the inhomogeneity of the ice. While it is considered likely that water is present within the ice at meteorite stranding sites, this is an assumption that may require testing in the field. Further, the cryoconites themselves, either formed from meteorites or from dust or other debris, will produce clutter in the radar signal. If the cryoconites are separated by more than a meter they will produce minimal clutter in the radar return in the region of interest (down to 1m), however if they are more closely spaced then the clutter could cause false detections and generally make the signal processing task more difficult. It is impossible

to assess the impact of sub-surface clutter without a better understanding of the situation, which may be best achieved by doing a trial at a potential stranding site where cryoconites are present.

Surface Clutter

A typical target range in subsurface radar is not large compared with the resolution distance as set by the transmitted bandwidth: factors of greater than 20 are rarely encountered, and they can be as low as 1 or 2. In our example the range used for calculation purposes, 1meter, is 6 times the vertical resolution, however in reality it will vare and will often be lower. Consequently, any breakthrough signal between transmit and receive antennas is either very close in time to the received signal from a shallow target. The breakthrough signal is one source of clutter encountered in GPR; that is, a component of the received signal which is present because of the fact of transmission of some waveform, and which cannot be removed by time-averaging the received signal (21). Detection of meteorites under thin layers of surface snow is thus not possible using GPR.

Initial Considerations of the Use of Magnetometers

The disadvantage is that they will only detect meteorites with electromagnetic properties sufficiently different from the ice. Two important features for detection by Electromagnetic methods are the electrical conductivity, magnetic susceptibility and the remnant magnetism. Ranges of magnetic susceptibility ranges are shown on Fig 3 of (8). The metallic meteorites (a natural Nickel-Iron alloy) will have a very large magnetic susceptibility, however these are not in the majority and it would be highly limiting to restrict the instrument to detecting only this type of meteorite.

The following references give an indication of the electrical conductivity of chondritic meteorites. (1) and (6) state that the electrical conductivity of chondrite meteorites (the most common meteorite composition type) can vary by a factor of 10^5, and are typically 4 to 6 order of magnitude greater than rock forming minerals such as Olivine. (7) gives a list of conductivities for carbonaceous meteorites between 10^{-3} and 10^{-10} $(ohm.cm)^{-1}$.

The detection limit for instruments that detect conductivity depend on the contrast with the bulk conductivity of ice, which is 5.5×10^{-4} $(ohm.cm)^{-1}$. Similarly methods that detect effects of the dielectric constant require contrast compared to that of ice at 3.17 and snow at 2.0.

Another possible detection method is paramagnetic or remnant or magnetization. The natural remnant magnetization was reported in (11) for a sample of 22 ordinary chondrite meteorites (types E, H L and LL), measured to be between 7.9E-5 and 2.8E-1 Am^2/kg. This might be picked up with a highly sensitive magnetometer.

The contrasts in electromagnetic properties between ice and a large fraction of meteorites indicate that this method of detection may be feasible and deserves greater study. There is

also a difference, though smaller, between the electromagnetic properties of terrestrial rocks and meteorites, giving the possibility for differentiation that could significantly reduce false positives. Furthermore, it would be simpler to implement a line of magnetometers on a boom trailing a skidoo than it is to implement a line of GPR transmitters and receivers, due to size and power requirements.

Discussion

The analysis presented here shows that it should be quite feasible to use of GPR to detect meteorites, especially where they are buried in homogenous ice. One of the major issues that has not been considered in this study is the presence of terrestrial rocks in many meteorite stranding sites. It has been observed that many meteorite stranding surfaces are rich in terrestrial rock, which will produce an unacceptably large number of false positives.

Further investigation of the scattering cross-section is recommended. While this should be initially calculated based on the properties of the meteorites and the ice, it will remain somewhat inconclusive until an experiment is performed. It is also recommended that sub-surface clutter effects be investigated by taking measurements in indicative sites in the field.

GPR can not detect meteorites at the very-near surface due to clutter. Magnetometers may be a better detection method as the electromagnetic properties of most meteorites are sufficiently different from both ice and from terrestrial rock, and deserve further study. However a search that is rejecting all targets with electromagnetic characteristics that match terrestrial rocks will inevitably miss that subset of meteorites. This will have the effect of skewing the meteorite population statistics and will introduce a risk of erroneous conclusions being drawn about the characteristics of the source asteroid population.

Extraction of meteorites at any depth in solid ice may be difficult and time-consuming, and may make the detection of sub-surface meteorites irrelevant. Again, some experimentation is the best method of resolving this issue.

Conclusions

While it is concluded that the GPR will allow the detection of large numbers of meteorites that are currently going unnoticed, it is also noted that the search efficiency and collection rates would likely not improve using these technologies, and thus they are unlikely to be implemented in the near future.

Magentometer systems deserve further study as a potential tool to increase detection rates, though this comes at the risk of skewing the collection population in favor of meteorites with larger differences in electromagnetic properties.

Acknowledgements

I would like to thank Jack Baggaley for setting me on the right path to find the material, and Wolfgang Rack for explaining certain aspects of GPR. This study would not have been possible without the support of the staff of Gateway Antarctica.

References:

(1) The Meteoritical Bulletin Database, http://www.lpi.usra.edu/meteor/metbull.php, (retrieved 15 February 2011), incorporating all published meteorites up to and including *Meteoritical Bulletin 99*.

(2) van den Broeke, M., van de Berg, W.J., van Meijgaard, E., and Reijmer, C., 2006, Identification of Antarctic ablation areas using a regional atmospheric climate model, Journal Of Geophysical Research, vol. 111

(3) Harvey, R., 2003, *The origin and significance of Antarctic meteorites*. Chemie der Erde 63 (2): 93–147

(4) Apostolopoulos, D.S.; Pedersen, L.; Shamah, B.N.; Shillcutt, K.; Wagner, M.D.; Whittaker, W.L.; 2001, *Robotic Antarctic meteorite search: outcomes*, Robotics and Automation, Proceedings 2001 ICRA. IEEE International Conference on , vol.4, no., pp. 4174- 4179 vol.4

(5) Lewis, J.S., *Physics and chemistry of the solar system*, 2nd Ed, 2004, Elservier

(6) Duba, Al, et al., 1987, *Electrical conductivity of chondritic meteorites*, in NASA, Lyndon B. Johnson Space Center, Experiments in Planetary and Related Sciences and the Space Station 2 p (SEE N89-14998 06-88)

(7) Brecher, A., Briggs, P.L., Simmons, G., 1975, *The low-temperature electrical properties of carbonaceous meteorites*, Earth and Planetary Science Letters, Volume 28, Issue 1, Pages 37-45

(8) A. ElkShoulder1 et. al, *Meteorite Identification And Classification Using Magnetic Susceptibility*, Lunar and Planetary Science XXXVII (2006)

(9) Moorehead, S., *Specification and Functionality of the Science Autonomy System for the 1998 Antarctic Field Season*, Version 1.2 November 4, 1998

(10) P. Lee, W.A. Cassidy, D. Apostolopoulos, D. Bassi, L. Bravo, H. Cifuentes, M. Deans, A. Foessel, S. Moorehead, M. Parris, C. Puebla, L. Pedersen, M. Sibenac, F. Valdés, N. Vandapel, and W.L. Whittaker, *Search for Meteorites at Martin Hills and Pirrit Hills Antarctica*, Lunar and Planetary Science Conference XXX, 1999.

(11) Brecher, A., and Ranganayaki, R.P., *Paleomagnetic Systematics Of Ordinary Chondrites*, Earth and Planetary Science Letters, 25 (1975) 57-67

(12) Folco, L; Rochette, P; Gattacceca, J; Perchiazzi, N, *In situ identification, pairing, and classification of meteorites from Antarctica through magnetic susceptibility measurements*, Meteoritics & Planetary Science, Volume 41, Issue 3, Pages 331-489 (March 2006) , pp. 343-353(11)

(13) Schwander, J., Neflel, A., Oeschger, H., and Stauffer B., 1983, *Measurement of Direct Current Conductivity on Ice Samples for Climatological Applications*, J. Phys. Chem., 87, 4157-4160 4157

(14) Kevin O'Neill, 2000, Radar Sensing of Thin Surface Layers and Near-Surface Buried Objects, IEEE Transactions on Geoscience & Remote Sensing, vol. 38, no. 1

(15) Salem, A., and Ushijima, K., 2001, *Automatic Detection of UXO from Airborne Magnetic Data Using a Neural Network*, Subsurface Sensing Technologies and Applications Vol. 2, No. 3

(16) Davis, K.C., Sandness, G. A., 1994, *A New Ground-Penetrating Radar System For Remote Site Characterization*, Fifth International Symposium on Robots & Manufacturing, Maui, HI (United States),14-18 Aug 1994

(17) Basson, U., 2000. *Imaging of active fault zone in the Dead Sea Rift: Evrona Fault Zone as a case study*. Thesis submitted for the degree of Ph.D., Tel-Aviv University, Raymond & Beverly Sackler, Faculty of Exact Sciences, Department of Geophysics & Planetary Sciences

(18) Rial, F.I., Lorenzo, H., Pereira, M. and Armesto, J., 2009, *Waveform Analysis of UWB GPR Antenna*s, Sensors, Vol. 9, 1454-1470

(19) Sensors & Software Inc. 1999, *Ground Penetrating Radar Survey Design*, Application note.

(20) Davis, J.L. and Annan, A.P. 1989. Ground-penetrating radar for high-resolution mapping of soil and rock stratigraphy. Geophysical Prospecting 37, 531-551

(21) Daniels, D.J.; Gunton, D.J. and Scott, H.F., 1988. Introduction to subsurface radar. IEE Proceedings, 135, part F, no. 4, 277-320

(22) *Electronic Warfare and Radar Systems Handbook*, 1999, Naval Air Systems Command and Naval Air Warfare Center, United States of America

(23) Yuan, Y., Chan, C.H., and Man, K.F., 2004, *Broadband Impedance Compensation for Ground Penetration Radar Antenna Using Genetic Algorithms,* 2004 IEEE International Antennas and Propagation Symposium Digest, Vol 1, Monterey, USA, 20-26 June 2004, pp 866-869

(24) B.K. Chung and T.P. Lee, 2008, *UWB Antenna Assists Ground-Penetrating Radar*, Microwaves and RF, pp. 59-65, December 2008.

(25) Chen, T.LG., 2006, *GPR Propagation Simulation and Fat Dipole Antenna Design*, Masters Thesis, University of Cape Town

(26) Turk, A.S., 2006, *Ultra-wideband Vivaldi antenna design for multisensor adaptive ground-penetrating impulse radar*, Microwave and Optical Technology Letters, vol 48, pp. 834-839

(27) Turk, A.S. and Nazil H., 2008, *Hyper-Wide Band TEM Horn Array Design for Multi Band Ground- Penetrating Impulse Radar*, Microwave And Optical Technology Letters, vol 50, pp. 76-81

(28) Turk, A. S. Sahinkaya, D. A. Sezgin, M. Nazli, H., 2007, *Investigation of Convenient Antenna Designs for Ultra-Wide Band GPR Systems*, Advanced Ground Penetrating Radar, 2007 4th International Workshop on, pp. 192-196

(29) Azodi, H., 2010, *UWB Air-Coupled Antenna for Ground Penetrating Radar*, Masters Thesis, Delft University of Technology

(30) Congedo, F., Monti, G., Tarricone, L., 2010, *Modified bowtie antenna for GPR applications*, Ground Penetrating Radar (GPR), 2010 13th International Conference on , vol., no., pp.1-5

(31) Blog of the Antarctic Search for Meteorites 2006/2007, http://www.humanedgetech.com/expedition/ansmet2/

(32) Annan, A.P., and Davis, J.L., 1976, *Impulse radar sounding in permafrost*. Radio Science, vol. 11, no. 4, pp. 383-394

(33) Koh, G., 1997, *Complex dielectric constant of ice at 1.8 GHz*, Cold Regions Science and Technology, Vol. 25, pp. 119–121

(34) Matzler, C., and Wegmuller, U., 1987, *Dielectric Properties of fresh-water ice at microwave frequencies*, Journal of Physics D: Applied Physics, vol. 20, pp. 1623-1630

(35) Warren, S.G., 1984, *Optical constants of ice from the ultraviolet to the microwave*, Applied Optics, Vol. 23, Iss. 8, pp. 1206–1225

(36) Prokhorenko, V., 1997, *An Impulse Generator For The Ground Penetrating Radar*, 12th International Congress of Speleology, La Chaux-De-Fonds, Switzerland.

(37) Prokhorenko, V., Boryssenko, A., 2000, *Drift Step Recovery Diode Transmitter for High Power GPR Design*, Eighth International Conference on Ground Penetration Radar, Gold Coast, Australia, pp. 277-281

(38) Prokhorenko, V.P.; Ivashchuk, V.E.; Korsun, S.V., Ultrawideband and Ultrashort Impulse Signals, 2004 Second International Workshop

(39) Dolphin, L., 1990, *Ground-Penetrating Radars And Unexploded Ordinance*, International Radar Consulnatnts, Inc, http://ldolphin.org/GPROrds.html, retrieved 2 February 2011.

(40) Stillman D.E., Grimm, R.E., 2008, *Electrical Properties of Ice and Implications for Solar System Exploration*, 39th Lunar and Planetary Science Conference, 10-14 March, League City, Texas

(41) Maidique, M.A., von Hippel, A. and Westphal, W. B., 1971, *Transfer of Protons through "Pure" Ice fA Single Crystals. * III. Extrinsic versus Intrinsi Polarization; Surface versus Volume Conduction c*, Journal Of Chemical Physics, vol. 54, no. 1, pp 150-160

(42) Koh, G., 1997, *Dielectric properties of ice at millimeter wavelengths*, Geophysical Research Letters, vol. 24, no. 18, pp. 2311-2313

(43) Zhao, Y., Chen, Y., Tong, L., Zhong, L. and Jia, M., 2008, *The Measurement On The Dielectric Properties Of Fresh-Water Ice With Rectangular Waveguide At 2.6ghz-3.9ghz*, 2008 IEEE Geoscience and Remote Sensing Symposium

(44) Cumming, W.S., 1952, The Dielectric Properties of Ice and Snow at 3.2 Centimeters, Journal of Applied Physics, vol. 23, no. 7, pp 768 -773

(45) Gribbon, P.W.F., 1979, *Cryoconite holes on Sermikavasak, West Greenland*, Journal of Glaciology, vol 22, pg 177-181